Laser-field effects on the interaction of charged particles with a degenerate electron gas

N. R. Arista*
Centro Atómico Bariloche, División Colisiones Atómicas, 8400 Bariloche, R.N., Argentina

R. O. M. Galvão
Laboratorio Associado de Plasmas, Instituto de Pesquisas Espaciais, Caixa Postal 515, São José dos Campos, São Paulo, Brazil

L. C. M. Miranda
Laboratorio Associado de Sensores, Instituto de Pesquisas Espaciais, Caixa Postal 515, São José dos Campos, São Paulo, Brazil

(Received 21 March 1989)

We formulate a general description of the inelastic interaction between charged particles and a degenerate plasma in the presence of a strong laser field. The excitations in the plasma are described according to the random-phase-approximation formalism, in terms of the dielectric function of the medium, and including the effects of the laser field on the dynamical response. The energy exchange and the scattering rate of the particle in the plasma are modified by multiphoton processes. The formalism describes the excitation of plasmons and electron-hole pairs, with simultaneous emission or absorption of photons. We calculate the contribution of these processes to the energy-loss rate and to the mean free path of the particle in the range of solid-state densities. New effects due to the laser field are expected for intensities similar to those used in laser fusion experiments.

I. INTRODUCTION

The interaction of charged particles with a degenerate electron gas has been a subject of great activity, starting with the work of Bohm, Pines, Lindhard, Ritchie, and other authors.[1–3] A comprehensive treatment of the quantities related to inelastic particle-solid and particle-plasma interactions, like scattering rates and differential and total mean free paths and energy losses, can be formulated in terms of the dielectric response function obtained from the electron gas model. The results have important applications in radiation and solid-state physics,[4,5] and more recently, in studies of energy deposition by ion beams in plasma fusion targets.[6]

On the other hand, the achievement of high-intensity laser beams with frequencies ranging between the infrared and vacuum-ultraviolet region has given rise to the possibility of new studies of interaction processes, such as electron-atom scattering in laser fields,[7,8] multiphoton ionization,[9] inverse bremsstrahlung and plasma heating,[10,11] and other processes of interest for applications in optics, solid-state, and fusion research.

Here we present a study of the effects of strong laser fields on the interaction of fast nonrelativistic particles with a degenerate electron gas. The problem is formulated using the random-phase approximation (RPA), and includes the effects of the radiation field in a self-consistent way. The results are expressed in terms of the RPA dielectric function for quantum plasmas, $\epsilon(k,\omega)$, with frequencies associated to the harmonics of the laser frequency ω_0.

The electromagnetic field is treated in the long-wavelength limit, and the electrons are considered nonrelativistic. These are good approximations provided that (i) the wavelength of the laser field ($\lambda_0 = 2\pi c/\omega_0$) is much larger than the Thomas-Fermi screening length [$\lambda_{TF} = v_F/\sqrt{3}\omega_p$ (with v_F the Fermi velocity and ω_p the plasma frequency)], and (ii) the "quiver velocity" of the electrons in the laser field ($v_e = eE_0/m\omega_0$) is much smaller than the speed of light c.

These conditions can be written as

$$\text{(i)}\quad \frac{\omega_0}{\omega_p} \ll \frac{2\pi c}{v_F}\ ,$$
$$\text{(ii)}\quad I_L \ll \tfrac{1}{2} nc(mc^2)\left[\frac{\omega_0}{\omega_p}\right]^2\ , \tag{1}$$

where $I_L = cE_0^2/8\pi$ is the laser intensity. As an estimate in the case of Al, with conduction electron density $n = 1.8\times 10^{23}$ cm^{-3}, we get $nmc^3/2 \cong 2\times 10^{20}$ W/cm^2. Thus the limits (i) and (ii) are well above the values obtained with currently available high-power laser, and so the approximations are well justified.

The present formalism yields general expressions for the inelastic scattering rates, which include plasmon and single-particle excitations in the plasma, and single or multiphoton emission or absorption processes.

We calculate the effects of the laser field on the mean energy loss (stopping power) and on the mean free path for plasmon excitation, and discuss the results in terms of the probabilities for the various particle-plasma-laser interaction processes.

II. RPA FORMULATION

We start the calculation by writing the time-dependent Hamiltonian for the electrons in the presence of both a radiation field $\mathbf{A}(t)=(c/\omega_0)E_0\cos\omega_0 t$, and a self-consistent scalar field $\varphi(\mathbf{r},t)$, i.e.,[11]

$$H(t)=\sum_p \frac{1}{2m}\left[\mathbf{p}-\frac{e}{c}\mathbf{A}(t)\right]^2 c_p^\dagger c_p - e\sum_{p,k}\varphi(\mathbf{k},t)c_{p+k}^\dagger c_p \tag{2}$$

where $c_p, c_p^\dagger$ are annihilation and creation operators for electrons with momentum $\mathbf{p}$, and $\varphi(\mathbf{k},t)$ is the Fourier transform of $\varphi(\mathbf{r},t)$.

The field $\varphi(\mathbf{k},t)$ is produced by the external particle, of charge Ze and velocity $\mathbf{v}$, and by the induced electronic density, viz.,

$$k^2\varphi(\mathbf{k},t)=4\pi\rho(\mathbf{k},t)-4\pi e\sum_p \langle c_{p-k}^\dagger c_p\rangle_t \tag{3}$$

being $\rho(\mathbf{k},t)$ the Fourier transform of the particle charge density, $\rho(\mathbf{r},t)=Ze\delta(\mathbf{r}-\mathbf{v}t)$.

The time evolution of the operator $\langle c_{p-k}^\dagger c_p\rangle_t$ can be obtained from the equation

$$i\hbar\frac{\partial}{\partial t}(c_{p-k}^\dagger c_p)=[c_{p-k}^\dagger c_p, H(t)] . \tag{4}$$

This yields, using Eq. (2),

$$\frac{\partial}{\partial t}\langle c_{p-k}^\dagger c_p\rangle - \frac{i}{\hbar}(\tilde{\varepsilon}_{p-k}-\tilde{\varepsilon}_p)\langle c_{p-k}^\dagger c_p\rangle = \frac{ie}{\hbar}\varphi(\mathbf{k},t)(f_{p-k}-f_p) . \tag{5}$$

Here $f_p\equiv f(\mathbf{p})$ is the equilibrium distribution function for the degenerate electron gas (in our case the zero-temperature Fermi-Dirac distribution), and

$$\tilde{\varepsilon}_p(t)=\left[\mathbf{p}-\frac{e}{c}\mathbf{A}(t)\right]^2\Big/2m . \tag{6}$$

For a general time-dependent field $\mathbf{A}(t)$ Eq. (5) has the solution[11]

$$\langle c_{p-k}^\dagger c_p\rangle_t=\frac{ie}{\hbar Q(t)}(f_{p-k}-f_p)\int_{-\infty}^{t} dt'\varphi(\mathbf{k},t')Q(t') \tag{7}$$

with

$$Q(t')=\exp\left[-\frac{i}{\hbar}\int_{-\infty}^{t'} dt''[\tilde{\varepsilon}_{p-k}(t'')-\tilde{\varepsilon}_p(t'')]\right] \tag{7'}$$

and in particular, for an oscillatory field $\mathbf{A}(t)=\mathbf{A}_0\cos\omega_0 t$, with $\mathbf{A}_0=c\mathbf{E}_0/\omega_0$, we obtain

$$\langle c_{p-k}^\dagger c_p\rangle_t=\frac{ie}{\hbar}(f_{p-k}-f_p)\int_{-\infty}^{t} dt'\varphi(k,t')\exp\left[\frac{-i}{\hbar}(\varepsilon_p-\varepsilon_{p-k})(t-t')\right]\exp[-i\mathbf{k}\cdot\mathbf{a}(\sin\omega_0 t-\sin\omega_0 t')] \tag{8}$$

where $\mathbf{a}=e\mathbf{E}_0/m\omega_0^2$ is the transverse oscillation amplitude of the electrons driven by the electromagnetic field (quiver amplitude).

Finally, using Eq. (3) and making a further Fourier transform we obtain a solution for the field φ in the form

$$\tilde{\varphi}(\mathbf{k},\omega)\left[1+\frac{4\pi e^2}{\hbar k^2}\sum_p\frac{f_{p-k}-f_p}{\omega-(\varepsilon_p-\varepsilon_{p-k})/\hbar+i\delta}\right]=\frac{4\pi}{k^2}\tilde{\rho}(\mathbf{k},\omega) \tag{9}$$

where we introduced the frequency transforms $\tilde{\varphi}(\mathbf{k},\omega)$, $\tilde{\rho}(\mathbf{k},\omega)$ of the quantities

$$\begin{aligned}\tilde{\varphi}(\mathbf{k},t)&=\varphi(\mathbf{k},t)\exp(i\mathbf{k}\cdot\mathbf{a}\sin\omega_0 t) ,\\ \tilde{\rho}(\mathbf{k},t)&=\rho(\mathbf{k},t)\exp(i\mathbf{k}\cdot\mathbf{a}\sin\omega_0 t) .\end{aligned} \tag{10}$$

The term within large parentheses in Eq. (9) can be identified with the RPA expression for the dielectric function $\epsilon(k,\omega)$.

In the case of a particle with velocity $\mathbf{v}$, $\rho(\mathbf{r},t)=Ze\delta(\mathbf{r}-\mathbf{v}t)$ we find

$$\tilde{\rho}(\mathbf{k},\omega)=2\pi Ze\sum_{n=-\infty}^{\infty} J_n(\mathbf{k}\cdot\mathbf{a})\delta(\omega-\mathbf{k}\cdot\mathbf{v}+n\omega_0) \tag{11}$$

and using Eq. (9) we finally obtain, for the self-consistent field $\varphi(\mathbf{r},t)$,

$$\varphi(\mathbf{r},t)=\frac{Ze}{2\pi^2}\int d^3k\sum_{m,n}J_m(\mathbf{k}\cdot\mathbf{a})J_n(\mathbf{k}\cdot\mathbf{a})\times\frac{e^{i\mathbf{k}(\mathbf{r}-\mathbf{v}t)}e^{i(n-m)\omega_0 t}}{k^2\epsilon(k,\mathbf{k}\cdot\mathbf{v}-n\omega_0)} . \tag{12}$$

The result represents the dynamical response of the medium to the motion of the test particle in the presence of the laser field; it takes the form of an expansion over all the harmonics of the laser frequency, with coefficients $J_n(\mathbf{k}\cdot\mathbf{a})$ that depend on the intensity $I_L\propto a^2$.

III. ENERGY LOSS AND STOPPING POWER

From Eq. (12) it is straightforward to calculate the electric field $\mathbf{E}(\mathbf{r},t)=-\nabla\varphi(\mathbf{r},t)$, and the time average of the stopping field $\mathbf{E}_s=\langle\mathbf{E}(\mathbf{v}t,t)\rangle$ acting on the particle. Then, the mean energy-loss rate of the test particle becomes

$$\left\langle\frac{dE}{dt}\right\rangle=Ze\mathbf{v}\cdot\mathbf{E}_s=\frac{(Ze)^2}{2\pi^2}\int d^3k\frac{(\mathbf{k}\cdot\mathbf{v})}{k^2}\times\sum_{n=-\infty}^{\infty}J_n^2(\mathbf{k}\cdot\mathbf{a})\mathrm{Im}\left[\frac{-1}{\epsilon(k,\Omega_n)}\right] \tag{13}$$

with $\Omega_n = \mathbf{k}\cdot\mathbf{v} - n\omega_0$.

To illustrate the effects of the laser field we first consider the calculation of the stopping power $S = \langle dE/dx \rangle = v^{-1}\langle dE/dt \rangle$. It is convenient to take into account the symmetry of the integrand in Eq. (13), with respect to the change $\mathbf{k}, n \to -\mathbf{k}, -n$: $\mathrm{Im}[-1/\epsilon(k, \Omega_n)]$ changes sign, as well as the factor $\mathbf{k}\cdot\mathbf{v}$. Using also the property

$$J_n^2(x) = J_{-n}^2(x) \tag{14}$$

we obtain

$$S = \frac{(Ze)^2}{2\pi^2 v}\int d^3k \frac{(\mathbf{k}\cdot\mathbf{v})}{k^2}\left[J_0^2(x)\mathrm{Im}\left[\frac{-1}{\epsilon(k,\mathbf{k}\cdot\mathbf{v})}\right] + 2\sum_{N=1}^{\infty} J_N^2(x)\mathrm{Im}\left[\frac{-1}{\epsilon(k,\Omega_N)}\right]\right] \tag{15}$$

with $x = \mathbf{k}\cdot\mathbf{a}$, $\Omega_N = \mathbf{k}\cdot\mathbf{v} - N\omega_0$.

Hence, the stopping power depends on the particle velocity $\mathbf{v}$, and on the frequency ω_0 and intensity $I_L = cE_0^2/8\pi$ of the laser (the intensity dependence is given through the quiver amplitude $a = eE_0/m\omega_0^2$). Moreover, since the vector $\mathbf{k}$ in Eq. (15) is spherically integrated, S becomes also a function of the angle α between the velocity $\mathbf{v}$ and the direction of polarization of the laser field, represented by $\mathbf{a}$.

By comparison, the stopping power in the absence of laser field is given by

$$S_0 = \frac{(Ze)^2}{2\pi^2 v}\int d^3k \frac{(\mathbf{k}\cdot\mathbf{v})}{k^2}\,\mathrm{Im}\left[\frac{-1}{\epsilon(k,\omega)}\right]\Bigg|_{\omega=\mathbf{k}\cdot\mathbf{v}} . \tag{16}$$

In order to calculate the terms in Eq. (15), we illustrate in Fig. 1 the map of excitations in the ω-k plane for a degenerate electron gas, and the integration ranges for the cases $N = 0, 1, 2$. The excitations are represented by the energy-loss function $\mathrm{Im}[-1/\epsilon(k,\omega)]$ according to the expressions for the degenerate electron gas.[2] Since $\mathrm{Im}[-1/\epsilon(k,\omega)]$ is an odd function of the frequency ω, the map of excitations is symmetric with respect to the $\mathbf{k}$ axis.

The lines marked $A1, B1$ indicate the sharp resonances due to plasmon excitation.[12] The frequency of these modes ω_k is given by the dispersion relation: $\epsilon(k,\omega_k) = 0$, or to lowest order in k^2: $\omega_k^2 = \omega_p^2 + \frac{3}{5}k^2 v_F^2$, where $\omega_p^2 = (4\pi ne^2/m)^{1/2}$ is the usual plasma frequency.

The dashed regions denoted by A2 and B2 in Fig. 1 correspond to single-particle excitations or electron-hole pairs (i.e., excitations of electrons from the Fermi sphere), and are bound by the lines $\omega = \pm\omega_{1,2}$, with[12] $\omega_{1,2} = \hbar k^2/2m \mp k v_F$.

Next we consider the regions of integration in the ω-k plane for the various terms in Eq. (15). The range of frequencies of interest is determined by the dependence $\epsilon(k, \mathbf{k}\cdot\mathbf{v} - N\omega_0)$. Therefore the integration range for the Nth term is given by

$$-kv - N\omega_0 < \omega < kv - N\omega_0 . \tag{17}$$

Figure 1 shows these limits for $N = 0,1,2$, with dashed, dash-dotted, and dash-double-dotted lines. The origin of integration is displaced from $\omega = 0$ (for $N = 0$), to $\omega = -\omega_0$ (for $N = 1$), $\omega = -2\omega_0$ (for $N = 2$), and so on.

For a physical interpretation of the various cases we show in the right-hand side of Fig. 1 the diagrams of the corresponding inelastic processes. In general, we observe that the range $\omega > 0$ corresponds to processes accompanied by photon emission, whereas the range $\omega < 0$ corresponds to photon absorption, and $N = |n|$ is the number of photons involved in the process. Since the formalism describes two kinds of elementary excitations in the plasma the scattering can give place to either plasmons

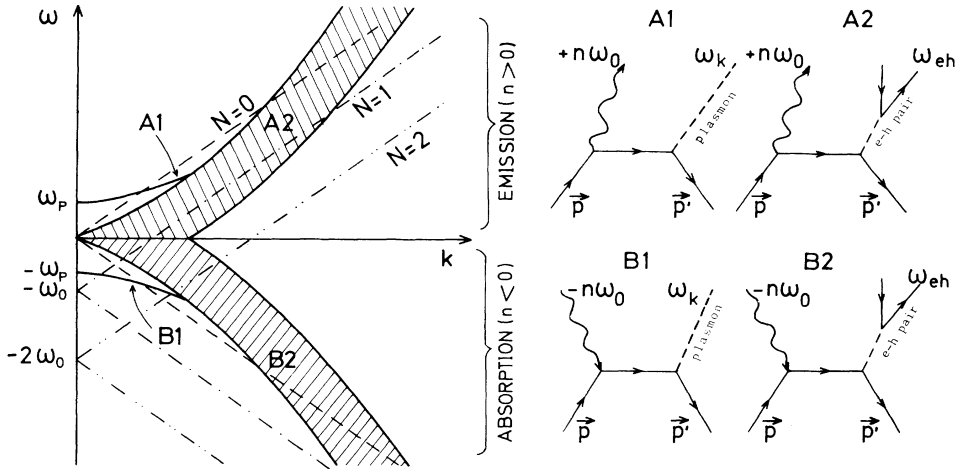

FIG. 1. Map of excitations in the ω-k plane (left side) for an electron gas in the presence of a laser field. The lines A1,B1 represent the excitation of plasmons with energy $\hbar\omega_k$, accompanied by emission or absorption of n photons. The dashed regions A2, B2 correspond to excitations of electron-hole pairs with energy $\hbar\omega_{eh}$, and simultaneous emission or absorption of n photons. These processes are illustrated by the diagrams on the right.

(lines A1, B1), or electron-hole pairs (regions A2,B2). Each of these processes is represented by the corresponding diagram in the right-hand side of Fig. 1.

IV. DERIVATION OF THE MEAN FREE PATH

To derive the expression for the mean free path (MFP) and scattering rate we note that Eq. (13) is of the form

$$\left\langle \frac{dE}{dt} \right\rangle = \int d^3k \, \Delta E_k \left[\frac{dP}{d^3k} \right] , \tag{18}$$

where $\Delta E_k = \hbar \mathbf{k} \cdot \mathbf{v}$ is the energy transfer in the scattering of a "heavy" particle (recoil terms are neglected) interacting inelastically with the plasma, and dP/d^3k is the differential probability for particle-plasma scattering with momentum transfer $\hbar \mathbf{k}$, and energy transfer ΔE_k, in the presence of the laser field.

From this relation we can derive the value of dP/d^3k. However, we should first collect the terms of Eq. (13) in such a way to obtain always positive scattering probabilities.

In the RPA formulation of Sec. II the electromagnetic field was considered as a classical quantity, while the system (electron gas) was treated quantum mechanically. This agrees with the semiclassical radiation theory approach. In addition, in this description the test particle was also considered as a classical external source. The result for the energy-loss rate $\langle dE/dt \rangle$, Eq. (13), becomes an integral over the frequency range described in Fig. 1. However, in calculating the probabilities for quantum-mechanical processes of inelastic scattering, the frequency ω in $\epsilon(k,\omega)$ represents also the energy transferred to the plasma ($\hbar\omega$) in the scattering event.

The function $\mathrm{Im}[-1/\epsilon(k,\omega)]$ appearing in Eq. (13) (usually called the energy-loss function) is odd with respect to ω, and therefore it can contribute with positive and negative terms to the integral. Hence, for a correct definition of (positive) scattering probabilities, we will describe the energy absorption by the function

$$F_0(k,\omega) = \begin{cases} \mathrm{Im}[-1/\epsilon(k,\omega)], & \omega > 0 \\ 0, & \omega < 0 \end{cases} \tag{19}$$

corresponding to a system that can only absorb energy.

The integral in Eq. (13),

$$X_n = \int d^3k \frac{(\mathbf{k}\cdot\mathbf{v})}{k^2} J_n^2(\mathbf{k}\cdot\mathbf{a}) \mathrm{Im} \left[\frac{-1}{\epsilon(k,\Omega_n)} \right] , \tag{20}$$

with $\Omega_n = \mathbf{k}\cdot\mathbf{v} - n\omega_0$, can be expressed in terms of the function $F_0(k,\omega)$ through the replacement

$$\mathrm{Im} \left[\frac{-1}{\epsilon(k,\Omega_n)} \right] = F_0(k,\Omega_n) - F_0(k,-\Omega_n) . \tag{21}$$

Then, for a given $m > 0$ we consider the contributions of both terms, with $n = \pm m$, viz.,

$$\begin{aligned} X_m &= \int d^2k \frac{(\mathbf{k}\cdot\mathbf{v})}{k^2} J_m^2(\mathbf{k}\cdot\mathbf{a}) \\ &\quad \times [F_0(k,\mathbf{k}\cdot\mathbf{v} - m\omega_0) - F_0(k,-\mathbf{k}\cdot\mathbf{v} + m\omega_0)] , \\ X_{-m} &= \int d^3k \frac{(\mathbf{k}\cdot\mathbf{v})}{k^2} J_{-m}^2(\mathbf{k}\cdot\mathbf{a}) \\ &\quad \times [F_0(k,\mathbf{k}\cdot\mathbf{v} + m\omega_0) - F_0(k,-\mathbf{k}\cdot\mathbf{v} - m\omega_0)] . \end{aligned} \tag{22}$$

By a parity transformation, $\mathbf{k} \leftrightarrow -\mathbf{k}$, in the second term of X_m we find

$$\begin{aligned} X_m &= \int d^3k \frac{(\mathbf{k}\cdot\mathbf{v})}{k^2} J_m^2(\mathbf{k}\cdot\mathbf{a}) \\ &\quad \times [F_0(k,\mathbf{k}\cdot\mathbf{v} - m\omega_0) + F_0(k,\mathbf{k}\cdot\mathbf{v} + m\omega_0)] . \end{aligned} \tag{23}$$

An identical result is obtained from X_{-m}, by the same transformation in the second term, and using that $J_m^2(x) = J_{-m}^2(x)$. Thus we get

$$\begin{aligned} (X_m + X_{-m}) &= 2 \int d^3k \frac{(\mathbf{k}\cdot\mathbf{v})}{k^2} J_m^2(\mathbf{k}\cdot\mathbf{a}) \\ &\quad \times [F_0(k,\mathbf{k}\cdot\mathbf{v} - m\omega_0) \\ &\quad + F_0(k,\mathbf{k}\cdot\mathbf{v} + m\omega_0)] . \end{aligned} \tag{24}$$

We can now separate from this integral the terms corresponding to photon emission,

$$2 \int d^3k \frac{(\mathbf{k}\cdot\mathbf{v})}{k^2} J_m^2(\mathbf{k}\cdot\mathbf{a}) F_0(k,\omega) \Big|_{\omega = \mathbf{k}\cdot\mathbf{v} - m\omega_0 > 0} , \tag{25}$$

and to photon absorption,

$$2 \int d^3k \frac{(\mathbf{k}\cdot\mathbf{v})}{k^2} J_{-m}^2(\mathbf{k}\cdot\mathbf{a}) F_0(k,\omega) \Big|_{\omega = \mathbf{k}\cdot\mathbf{v} + m\omega_0 > 0} , \tag{25'}$$

which in both cases have the correct behavior corresponding to real energy absorption by the electron gas (instead, the particle can gain or lose energy, depending on the energy exchange with the radiation field).

The scattering probability P, the MFP $\lambda \equiv 1/\mu$, and the mean scattering time τ, are related by $P = 1/\tau = v/\lambda$. Hence we define the differential inverse MFP (DIMFP) $d\mu_n$, and the inverse MFP (IMFP) μ_n, which according to Eqs. (13), (18), (25), and (25') take the form

$$d\mu_n = \frac{1}{v} dP_n = \frac{(Ze)^2}{\pi^2 \hbar v} \frac{d^3k}{k^2} J_n^2(\mathbf{k}\cdot\mathbf{a}) \mathrm{Im} \left[\frac{-1}{\epsilon(k,\Omega_n)} \right] \Big|_{\Omega_n > 0} , \tag{26}$$

$$\mu_n = \frac{(Ze)^2}{\pi^2 \hbar v} \int d^3k \frac{1}{k^2} J_n^2(\mathbf{k}\cdot\mathbf{a}) \mathrm{Im} \left[\frac{-1}{\epsilon(k,\Omega_n)} \right] \Big|_{\Omega_n > 0} . \tag{27}$$

These equations give the DIMFP and IMFP for the inelastic scattering of the particle in the plasma, with simultaneous absorption (if $n < 0$) or emission (if $n > 0$) of n photons of frequency ω_0.

As shown, the scattering rate dP_n, Eq. (26), is well defined only for $\Omega_n = \mathbf{k}\cdot\mathbf{v} - n\omega_0 > 0$. Therefore the regions of integration for the inverse mean free path are those shown in Fig. 2, where we illustrate only the particular

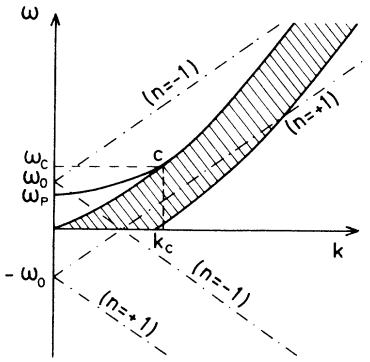

FIG. 2. Integration ranges for absorption ($n<0$) or emission ($n>0$) processes, according to the derivation of the scattering probabilities given in the text. They pertain to the same processes as Fig. 1, but the integration is restricted here to positive frequencies (see text for discussion).

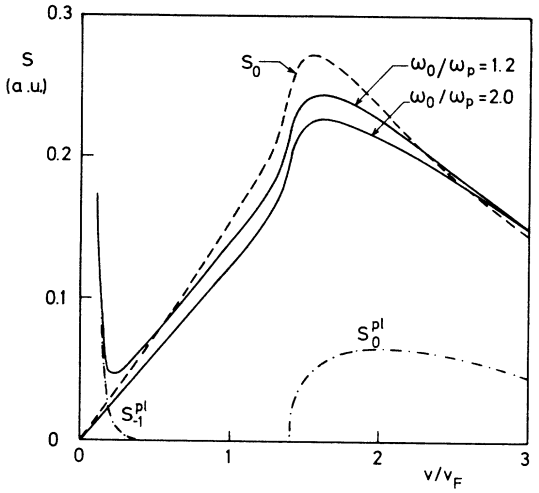

FIG. 3. Calculations of the stopping power for an electron gas with $\hbar\omega_p=15.5$ eV, at two laser frequencies, $\omega_0/\omega_p=1.2$ and 2.0, for $\omega_p a/v_F=0.5$. The dashed line shows the "normal" stopping power (in the absence of laser field). The contributions due to plasmon excitations are shown with dash-dotted lines for no-photon ($n=0$) and single-photon ($n=-1$) absorption. The low-velocity rise of the stopping power is due to the process of plasmon excitation assisted by photon absorption as discussed in the text.

cases with $n=\pm 1$.

The calculation of the MFP according to Eq. (27) is analogous to the stopping power integration, but the range of integration is restricted now to positive frequencies, whereas in the energy-loss integration of Fig. 1, both absorption and emission domains are mixed in an extended picture.

In fact, the integration over $\omega>0$ in Fig. 1 for $n=+1$ agrees exactly with the integration range for the emission term ($n=+1$) in Fig. 2, while the integration domain $\omega<0$ in Fig. 1, with $n=-1$, is the mirror image of the domain corresponding to the absorption process ($n=-1$) in Fig. 2. Hence both pictures become equivalent.

An alternative treatment of inelastic scattering processes, with absorption or emission of *single* photons (and simultaneous plasmon excitation), is given in the Appendix using perturbation theory and a simple model description of the plasmon field.

Here we note that the present expressions of $d\mu_n$ and μ_n are generalizations of those obtained in the Appendix in two important ways: (1) inclusion of multiphoton processes ($|n|>1$), of interest for very strong fields, and (2) self-consistent description of screening and dynamical-response effects through the properties of $\epsilon(k,\mathbf{k}\cdot\mathbf{v}-n\omega_0)$.

V. CALCULATIONS AND DISCUSSION

We show in Fig. 3 the results of stopping power calculations for an electron gas with $\hbar\omega_p=15.5$ eV, or $v_F=0.92$ a.u. (these values correspond to the conduction band of Al), for two laser frequencies, $\omega_0/\omega_p=1.2$ and 2.0, and for $\omega_p a/v_F=0.5$ (for the case of Al this corresponds to laser intensities $\sim 10^{16}$ W/cm^2). The line denoted $S_0^{\rm PL}$ is the energy loss due to plasmon excitation without the laser field, and has a threshold for $v/v_F=1.4$.

In general, we find that the effect of the laser field is to reduce the stopping power for velocities $v\sim v_F$, with respect to the stopping power without laser field (dashed line). However, for $\omega_0/\omega_p=1.2$ we observe a different behavior at low velocities, where there is an increase of the stopping power. We find that this effect is due to a different mechanism for plasmon excitation which arises when $\omega_0\cong\omega_p$, and below the "normal" velocity threshold.

The dependence of the stopping power on the angle α, between the velocity **v** and the direction of laser-field polarization, is shown in Fig. 4 for $v=v_F$.

In order to analyze the mechanism of plasmon excitation for low-velocity particles we show in Fig. 5, (a) the

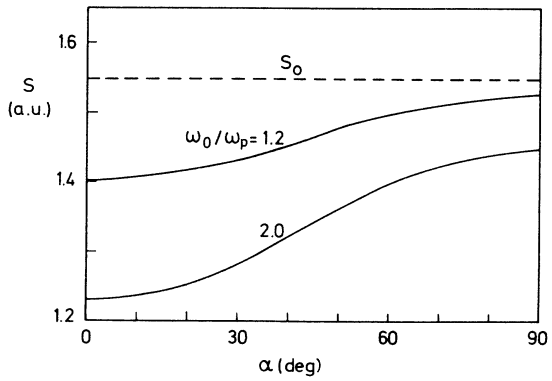

FIG. 4. Angular dependence of the stopping power at $v=v_F$, in terms of the angle α between the particle velocity **v** and the direction of polarization of the laser field $\hat{\epsilon}_0=\mathbf{E}_0/E_0$.

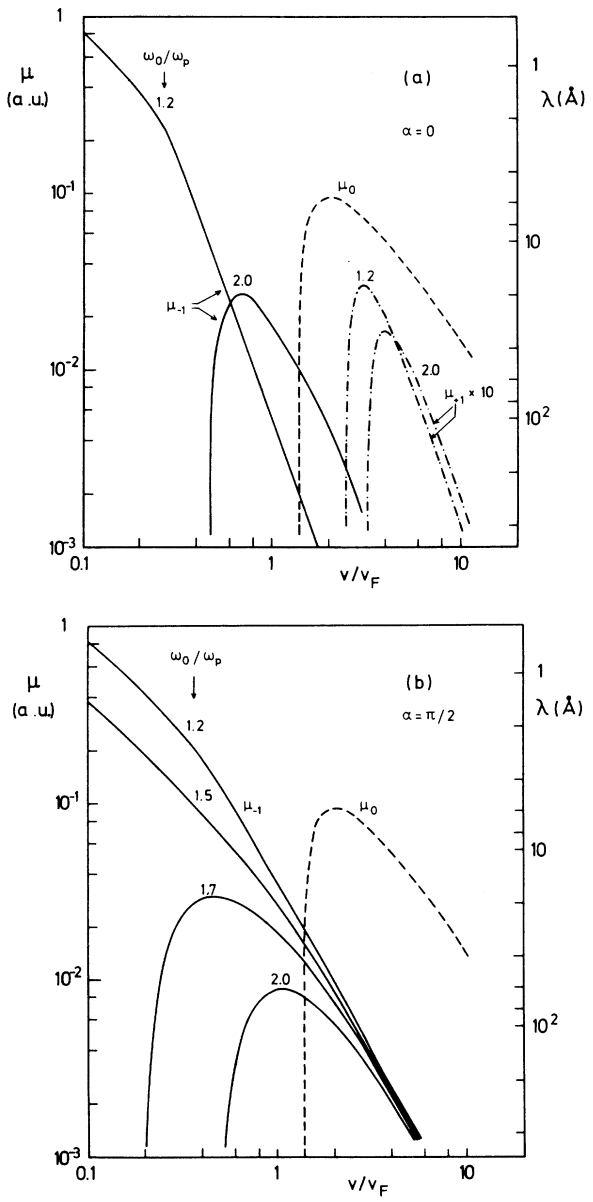

FIG. 5. Calculations of inverse mean free paths (IMFP) for plasmon excitation accompanied by single-photon absorption ($n=-1$, solid lines) and emission ($n=1$, dash-dotted lines), for laser frequencies in the range $\omega_0/\omega_p=1.2$ to 2.0, and for angles $\alpha=0$ (a) and $\pi/2$ (b). The line μ_0 is the "normal" IMFP (in the absence of laser field). The figure shows the shift and disappearance of the plasmon threshold when ω_0 approaches ω_p.

calculated inverse mean free path for plasmon excitation, $\mu_{\pm 1}$, for the two processes of first order with respect to the radiation field. Thus μ_{+1} corresponds to the process of particle scattering with emission of both a photon and a plasmon, while μ_{-1} represents the process of photon absorption accompanied by the emission of a plasmon. They are represented respectively by the diagrams A1 and B1 in Fig. 1 (with $n=\pm 1$ in this case). By comparison we also show the IMFP for "normal" plasmon excitation (i.e., in absence of laser field, dashed line).

We notice the strong increase in the probability for process B1 ($n=-1$) when ω_0 approaches ω_p. This behavior is further illustrated in 5(b), where we show the values of μ_{-1} for a set of ratios ω_0/ω_p.

To explain this effect, we consider the energy exchange by the particle in the process $n=-1$ (photon absorption with plasmon emission), given by (cf. the Appendix)

$$\Delta E_k^0=\hbar\mathbf{k}\cdot\mathbf{v}=k\omega_0-k\omega_k \ . \tag{28}$$

This indicates the possibility of energy *loss* (for $\omega_p<\omega_0<\omega_k$) or energy *gain* (for $\omega_0>\omega_k$) depending on the value of ω_0.

Due to plasmon dispersion effects, the value of ω_k lies in the range between ω_p and ω_c, cf. Fig. 2, where ω_c is the limiting plasmon frequency corresponding to a wave vector k_c such that plasmons start to decay into electron-hole pairs.[12]

Therefore, since plasmons are bound by $\omega_k<\omega_c$, and $k<k_c$, Eq. (28) gives a finite velocity threshold for process $n=-1$, namely,

$$v_{-1}=(\omega_0-\omega_c)/k_c \tag{29}$$

as long as $\omega_0>\omega_c$. When ω_0 is smaller than ω_c, the threshold velocity for this process becomes null. For the case considered here, $\omega_c/\omega_p\cong 1.5$, and so we see from Fig. 5 that for $\omega_0/\omega_p\leq 1.5$ there is no threshold for μ_{-1}. In this case there is a frequency range, $\omega_k\sim\omega_0$, which always contributes at low velocities, since the photon frequency is in resonance with some plasmon mode (in other words, part of the plasmon line will remain within the closing range between the two $n=-1$ lines of Fig. 2 for all smaller velocities).

VI. SUMMARY

We have developed a general formulation for the effects of strong laser fields on the inelastic interaction of swift particles with a quantum-mechanical plasma.

The RPA formulation, as extended in the presence of a laser field, provides a self-consistent description of the inelastic processes pertaining to particle-plasma-laser interactions. The formalism describes excitations of plasmons and electron-hole pairs, with simultaneous emission or absorption of photons. The interaction with the test particle provides a mechanism for energy transfer between the radiation and plasmon fields.

The scattering rates and the energy exchange are modified by single or multiphoton processes, depending on the laser-field intensity. Strong effects due to the laser field are found for intensities in the range of interest of laser fusion experiments.

For intermediate velocities, $v\sim v_F$, the laser produces in general a decrease of the stopping power. However, when the laser frequency ω_0 approaches the plasma frequency ω_p new effects arise in the range of low velocities ($v\ll v_F$). We describe the effects on the energy loss and inelastic mean free paths.

We find that the main contribution comes from the

process of plasmon excitation assisted by photon absorption; this occurs for velocities below the normal threshold for plasmon excitation, provided that ω_0 is within the range of plasmon dispersion frequencies ($\omega_p < \omega_0 < \omega_c$). In this case the threshold disappears and the energy of the absorbed photon is transferred to the plasmon field.

ACKNOWLEDGMENTS

This work was partially supported by the International Atomic Energy Agency (Vienna), and Consejo Nacional de Investigaciones Científicas y Técnicas (CONICET, Argentina).

APPENDIX: PERTURBATIVE CALCULATION OF SINGLE-PHOTON PROCESSES

We consider in this appendix an alternative derivation of the scattering rates for processes A1 and B1 ($n=\pm 1$) discussed in Secs. III–V, corresponding to single-photon emission or absorption. For this calculation we use a quantum-electrodynamical description of the photon and plasmon fields.

Hence we write the Hamiltonian for particle-plasma-laser interaction in the form

$$H = H_0 + H_1 \tag{A1}$$

where H_0 consists of the separate Hamiltonians of the radiation field, electron gas, and external particle, while the interaction Hamiltonian H_1 is given by[12,13]

$$H_1 = H_1^{\rm rad} + H_1^{\rm pl} + H_1^{\rm sr} \ . \tag{A2}$$

The first two terms correspond to the coupling between the particle and the radiation and plasmon fields, and are given by

$$H_1^{\rm rad} = \sum_{p,q} G_q (a_q + a^{\dagger}_{-q}) c^{\dagger}_{p+q} c_p (\mathbf{p}\cdot\hat{\boldsymbol{\epsilon}}_\alpha) \ , \tag{A3}$$

$$H_1^{\rm pl} = \sum_{p,k} g_k (b_k + b^{\dagger}_{-k}) c^{\dagger}_{p+k} c_p \ , \tag{A4}$$

where $\hbar\mathbf{q}$, $\hbar\mathbf{k}$, and $\hbar\mathbf{p}$ are the momenta of the photons, plasmons, and external particle, and a_q, b_k, and c_p are the respective annihilation operators; $\hat{\boldsymbol{\epsilon}}_\alpha$ is the polarization vector of the photons, and the coupling constants are

$$G_q^2 = \frac{2\pi\hbar}{V\omega_q^0}\left[\frac{e\hbar}{m}\right]^2 , \tag{A5}$$

$$g_k^2 = \frac{2\pi\hbar}{V\omega_k}\left[\frac{e\omega_p}{k}\right]^2 \tag{A5'}$$

where ω_q^0 and ω_k represent the photon and plasmon frequencies. In this case ω_q^0, $\mathbf{q}$, and $\hat{\boldsymbol{\epsilon}}_\alpha$ are given by the laser frequency ω_0, wave vector $\mathbf{q}_0$, and polarization vector $\hat{\boldsymbol{\epsilon}}_0$.

The term $H_1^{\rm sr}$ in Eq. (A2) accounts for the short-range coupling between the test particle and the electrons. This term gives place to electron-hole excitations (Fig. 1, diagrams A2, B2) and will not be discussed in this appendix.

Let us now calculate the matrix elements for the processes of plasmon excitation accompanied by spontaneous or stimulated photon emission, like those shown in Fig. 6.

The second-order matrix element for a transition between the initial $|a\rangle$ and the final state $|b\rangle$ is

$$M_{ab} = \sum_i \frac{\langle b|H_1|i\rangle\langle i|H_1|a\rangle}{E - E_i} \tag{A6}$$

(for the process under consideration the first-order term $\langle b|H_1|a\rangle$ gives no contribution).

In the case of diagram A1, the transition from $|a\rangle$ to the intermediate states $|i_1\rangle$ (containing a particle with momentum $\hbar\mathbf{p}_{i1}$ and a photon with momentum $\hbar\mathbf{q}_0$), is produced by the interaction term $H_1^{\rm rad}$, Eq. (A3), and yields

$$\langle i_1|H_1^{\rm rad}|a\rangle = G_{q_0}(N_0+1)^{1/2}(\mathbf{p}\cdot\hat{\boldsymbol{\epsilon}}_0) \tag{A7}$$

where N_0 is the number of photons with momentum $\hbar\mathbf{q}_0$ in the radiation field.

The second transition, from $|i_1\rangle$ to $|b\rangle$, given by the term $H_1^{\rm pl}$, yields

$$\langle b|H_1^{\rm pl}|i_1\rangle = g_k \ . \tag{A7'}$$

The energy and momentum of the intermediate state $|i_1\rangle$ are

$$\mathbf{p}_{i1} = \mathbf{p} - \mathbf{q}_0 = \mathbf{p}' + \mathbf{k} \ , \qquad E_{i1} = \hbar\omega_0 + \frac{\hbar^2}{2M}(\mathbf{p}-\mathbf{q}_0)^2 \tag{A8}$$

being M the mass of the particle.

In the same form, we calculate the matrix elements for the diagram A1′ in Fig. 6:

$$\langle i_2|H_1^{\rm pl}|a\rangle = g_k \ , \tag{A9}$$

$$\langle b|H_1^{\rm rad}|i_2\rangle = G_{q_0}(N_0+1)^{1/2}(\mathbf{p}'\cdot\hat{\boldsymbol{\epsilon}}_0) \tag{A9'}$$

with

$$\mathbf{p}_{i_2} = \mathbf{p} - \mathbf{k} = \mathbf{p}' + \mathbf{q}_0 \ , \qquad E_{i_2} = \hbar\omega_k + \frac{\hbar^2}{2M}(\mathbf{p}-\mathbf{k})^2 \ . \tag{A10}$$

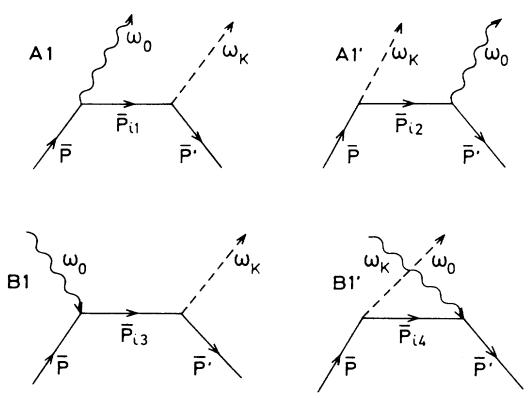

FIG. 6. Processes of lowest order with respect to the photon and plasmon fields, corresponding to the perturbative calculation of single-photon processes.

Therefore the total matrix element for plasmons excitation and single-photon emission, diagrams A1 and A1', becomes

$$M_{ab}^{(+1)}=g_k G_{q_0}(N_0+1)^{1/2}\left[\frac{\mathbf{p}\cdot\hat{\boldsymbol{\epsilon}}_0}{E-E_{i_1}}+\frac{\mathbf{p}'\cdot\hat{\boldsymbol{\epsilon}}_0}{E-E_{i_2}}\right] . \quad \text{(A11)}$$

This corresponds to the process with $n=+1$ of Sec. V.

In the same way we calculate the matrix elements for the diagrams B1, B1' of Fig. 6, namely,

$$\begin{aligned}
&\langle i_3|H_1^{\mathrm{rad}}|a\rangle=G_{q_0}(N_0)^{1/2}(\mathbf{p}\cdot\hat{\boldsymbol{\epsilon}}_0) ,\\
&\langle b|H_1^{\mathrm{pl}}|i_3\rangle=g_k ,\\
&\langle i_4|H_1^{\mathrm{pl}}|a\rangle=g_k ,\\
&\langle b|H_1^{\mathrm{rad}}|i_4\rangle=G_{q_0}(N_0)^{1/2}(\mathbf{p}'\cdot\hat{\boldsymbol{\epsilon}}_0)
\end{aligned} \quad \text{(A12)}$$

with

$$\begin{aligned}
&\mathbf{p}_{i_3}=\mathbf{p}+\mathbf{q}_0=\mathbf{p}'+\mathbf{k} ,\\
&\mathbf{p}_{i_4}=\mathbf{p}-\mathbf{k}=\mathbf{p}'-\mathbf{q}_0 ,\\
&E_{i_3}=\frac{\hbar^2}{2M}(\mathbf{p}+\mathbf{q}_0)^2 ,\\
&E_{i_4}=\hbar\omega_0+\hbar\omega_k+\frac{\hbar^2}{2M}(\mathbf{p}'-\mathbf{q}_0)^2 .
\end{aligned} \quad \text{(A13)}$$

Hence the matrix element becomes

$$M_{ab}^{(-1)}=g_k G_{q_0}(N_0)^{1/2}\left[\frac{\mathbf{p}\cdot\hat{\boldsymbol{\epsilon}}_0}{E-E_{i_3}}+\frac{\mathbf{p}'\cdot\hat{\boldsymbol{\epsilon}}_0}{E-E_{i_4}}\right] . \quad \text{(A14)}$$

This corresponds to the process of plasmon excitation with single-photon absorption, (i.e., the $n=-1$ term of Sec. V.

The terms within brackets in Eqs. (A11) and (A14) can still be reduced to a simpler form if the photon momentum is neglected (low-q approximation). This corresponds to the nonrelativistic approximation.

Thus neglecting terms of order v/c we obtain

$$\left[\frac{\mathbf{p}\cdot\hat{\boldsymbol{\epsilon}}_0}{E-E_i}+\frac{\mathbf{p}'\cdot\hat{\boldsymbol{\epsilon}}_0}{E-E_i'}\right]\cong\frac{\mathbf{k}\cdot\hat{\boldsymbol{\epsilon}}_0}{\hbar(\omega_k-\mathbf{k}\cdot\mathbf{v})} . \quad \text{(A15)}$$

The transition probability per unit time is given by the well-known expression

$$dW_{\pm1}=\frac{2\pi}{\hbar}|M_{ab}^{(\pm1)}|^2\frac{Vd^3k}{(2\pi)^3}\delta(E_p^0\mp\hbar\omega_0-E_{p'}^0-\hbar\omega_k) \quad \text{(A16)}$$

where $E_p^0=\hbar^2p^2/2M$ is the particle kinetic energy.

The energy difference $\Delta E_{ab}=E_p^0\mp\hbar\omega_0-E_{p'}^0-\hbar\omega_k$, in the low-$q$ approximation ($\mathbf{p}'\cong\mathbf{p}-\mathbf{k}$) becomes

$$\Delta E_{ab}^{(\pm1)}=\mp\hbar\omega_0-\hbar\omega_k+\frac{\hbar^2}{2M}[p^2-(\mathbf{p}-\mathbf{k})^2] . \quad \text{(A17)}$$

For a heavy particle (or a fast electron), we can neglect the particle recoil in the scattering process. Therefore the energy change by the particle is

$$\Delta E_k^0=\frac{\hbar^2}{2M}[p^2-(\mathbf{p}-\mathbf{k})^2]\cong\frac{\hbar^2}{2M}(2\mathbf{p}\cdot\mathbf{k})=\hbar\mathbf{v}\cdot\mathbf{k} . \quad \text{(A18)}$$

Hence

$$\Delta E_{ab}^{(\pm1)}\cong\hbar(\mathbf{k}\cdot\mathbf{v}\mp\omega_0-\omega_k) . \quad \text{(A19)}$$

Finally, using Eqs. (A16)–(A19), we obtain the probability for processes $n=\pm1$:

$$dW_{\pm1}=\frac{e^4\omega_p^2}{m^2\omega_0^3\omega_k}\left[\frac{N}{V}\right]\frac{(\mathbf{k}\cdot\hat{\boldsymbol{\epsilon}}_0)^2}{k^2}\delta(\mathbf{k}\cdot\mathbf{v}-\omega_k\mp\omega_0)d^3k \quad \text{(A20)}$$

with $N=N_0$ for $n=-1$ (photon absorption), and $N=N_0+1$ for $n=+1$ (photon emission).

This result can be compared with Eq. (26), obtained from the dielectric function formalism. The present perturbation analysis, for single-photon processes, applies for relatively low intensities of the laser field. Therefore in the limit of low laser intensities we approximate $J_1^2(\mathbf{k}\cdot\mathbf{a})\cong(\mathbf{k}\cdot\mathbf{a})^2/4$ in Eq. (26). Moreover we use the plasmon-pole approximation for the plasma resonance, viz.

$$\mathrm{Im}\left[\frac{-1}{\epsilon(k,\omega)}\right]\cong\frac{\pi}{2}\frac{\omega_p^2}{\omega_k}\delta(\omega-\omega_k) . \quad \text{(A21)}$$

Then, from Eq. (26), with $n=\pm1$, we get

$$dP_{\pm1}=\frac{e^2}{\pi^2\hbar}\frac{(\mathbf{k}\cdot\mathbf{a})^2}{4k^2}\frac{\pi}{2}\frac{\omega_p^2}{\omega_k}\delta(\Omega_{\pm1}-\omega_k)d^3k \quad \text{(A22)}$$

and since $\Omega_{\pm1}=\mathbf{k}\cdot\mathbf{v}\mp\omega_0$, $\mathbf{a}=eE_0\hat{\boldsymbol{\epsilon}}_0/m\omega_0^2$, we get

$$dP_{\pm1}=\frac{e^2}{8\pi\hbar}\frac{(\mathbf{k}\cdot\hat{\boldsymbol{\epsilon}}_0)^2}{k^2}\frac{e^2E_0^2}{m^2\omega_0^4}\frac{\omega_p^2}{\omega_k}\delta(\mathbf{k}\cdot\mathbf{v}\mp\omega_0-\omega_k)d^3k , \quad \text{(A23)}$$

which fully agrees with Eq. (A20), since the number of photons per unit volume is related to E_0 as $N/V=E_0^2/8\pi\hbar\omega_0$.

To conclude we note that while the RPA treatment given in Secs. III–V yields a more comprehensive description, the present approach provides a simple physical insight into the problem. In addition, both descriptions are equivalent for single-photon processes in the plasmon-pole approximation.

*Present address: Universitat d' Alacant, Departamento de Física Aplicada, Apt. 99, E-03080, Alicante, Spain.

[1]D. Bohm and D. Pines, Phys. Rev. **82**, 625 (1951); **85**, 338 (1952).

[2]J. Lindhard, K. Dan. Vidensk. Selsk., Mat.—Fys. Medd. **28**, No. 8 (1954); J. Lindhard and A. Winther, *ibid.* **34**, No. 4 (1964).

[3]R. H. Ritchie, Phys. Rev. **114**, 644 (1959).

[4]R. H. Ritchie, C. J. Tung, V. E. Anderson, and J. C. Ashley, Radiat. Res. **64**, 181 (1975); C. J. Tung and R. H. Ritchie,

Phys. Rev. B **16**, 4302 (1977).
[5]P. M. Echenique, Nucl. Instrum. Methods B **27**, 256 (1987).
[6]N. R. Arista and W. Brandt, Phys. Rev. A **23**, 1898 (1981); T. A. Mehlhorn, J. Appl. Phys. **52**, 6522 (1981); G. Maynard and C. Deutsch, *ibid.* **26**, 665 (1982); N. R. Arista and A. R. Piriz, *ibid.* **35**, 3450 (1987).
[7]N. M. Kroll and K. M. Watson, Phys. Rev. A **8**, 804 (1973).
[8]A. Weingartshofer *et al.*, Phys. Rev. Lett. **39**, 269 (1977); J. Phys. B **16**, 1805 (1983).
[9]L. A. Lompre *et al.*, Phys. Rev. Lett. **36**, 949 (1976); K. G. Baldwin and B. W. Boreham, J. Appl. Phys. **52**, 2627 (1981).
[10]J. F. Seely and E. G. Harris, Phys. Rev. A **7**, 1064 (1973); S. H. Kim and P. Y. Pac, *ibid.* **19**, 2139 (1979).
[11]M. B. S. Lima, C. A. S. Lima, and L. C. M. Miranda, Phys. Rev. A **19**, 1796 (1979).
[12]D. Pines, *Elementary Excitations in Solids* (Benjamin, New York, 1964).
[13]C. Kittel, *Quantum Theory of Solids* (Wiley, New York, 1963).